Forest Ecology and Management 537 (2023) 120945

Contents lists available at ScienceDirect

Forest Ecology and Management

journal homepage: www.elsevier.com/locate/foreco

Characterizing ground and surface fuels across Sierra Nevada forests shortly after the 2012–2016 drought

Emilio Vilanova[a,*], Leif A. Mortenson[b], Lauren E. Cox[c], Beverly M. Bulaon[d], Jamie M. Lydersen[e], Christopher J. Fettig[f], John J. Battles[a], Jodi N. Axelson[g]

[a] Department of Environmental Science, Policy, and Management, University of California, 130 Mulford Hall, Berkeley, CA 94720, USA
[b] Pacific Southwest Research Station, USDA Forest Service, 2480 Carson Road, Placerville, CA 95667, USA
[c] University of Nevada, N. Virginia Street, Reno, NV 89557, USA
[d] Forest Health Protection, USDA Forest Service, 19777 Greenley Road, Sonora, CA 95370, USA
[e] California Department of Forestry and Fire Protection, Fire and Resource Assessment Program, P.O. Box 944246, Sacramento, CA 94244, USA
[f] Pacific Southwest Research Station, USDA Forest Service, 1731 Research Park Drive, Davis, CA 95618, USA
[g] Forest Science, Planning and Practices Branch, British Columbia Ministry of Forests, P.O. Box 9513, Victoria, BC V8W 9C2, Canada

ARTICLE INFO

Keywords:
Bark beetle
California
Ground fuels
Forest management
Tree mortality
Wildfires

ABSTRACT

The 2012–2016 hotter drought in the Sierra Nevada, California, USA led to the mortality of millions of trees. This disruption to the disturbance regime is an example of how climate extremes can exacerbate current and future wildfire risks. In this study, we used data from an extensive network of forest plots across 13 different sites in the Sierra Nevada to characterize ground (i.e., duff) and surface fuels and their potential drivers shortly after the drought (2016–2018), but before snag (standing dead tree) fall associated with this massive tree mortality event occurred. Overall, we found high biomass of fuels for most sites (138.2 ± 21.7 Mg ha^{-1}, Mean ± 95 % CI), especially in areas lacking recent fire or active management, with values up to five times higher than estimates for pre-settlement conditions for mixed-conifer forests in the region. Four major groups of forest overstory structure were identified with some distinct fuel characteristics. These ranged from a cluster of ponderosa pine (*Pinus ponderosa* Douglas ex Lawson)-dominated plots with the highest density of snags, lowest live tree basal area, and lowest total ground and surface fuel biomass (mean = 90.1 Mg ha^{-1}) to a group of giant sequoia (*Sequoiadendron giganteum* (Lindl.) J. Buchholz)-dominated plots with the highest live tree basal area and highest total fuel biomass (mean = 547.6 Mg ha^{-1}). Although we found relatively weak relationships between forest characteristics and fuel loads, their inclusion in a model selection framework that also considered biophysical variables and disturbance history explained>80 % of the observed variation in litter + fine woody debris loads. The baseline fuel conditions described here will not only inform the management of drought-impacted forests in the Sierra Nevada, but also help identify key drivers of fuel succession in a changing environment.

1. Introduction

The disruption of forest disturbance regimes by global change poses a grave risk to the resilience of forest ecosystems (Seidl et al., 2016). Among the major disturbance agents, the climate-induced (*sensu* Seidl et al., 2017) increases in the extent, severity, and unpredictability of wildfires are perceived as a threat to human society (Kareiva and Carranza, 2018; Parks and Abatzoglou, 2020). In this regard, Gillson et al. (2019) argue that wildfire management in the Anthropocene must adapt to promote social-ecological resilience. A common charge from these reviews (Gillson et al., 2019; Seidl et al., 2016) is the need for an adaptive, learning-based approach to managing this and other shifts in the disturbance regime.

Unfortunately, the current condition of the vast conifer forests in the Sierra Nevada (California) provides a specific example of these global concerns. Decades of extensive fire exclusion and suppression, logging, grazing and expansion of the wildland-urban interface (Byer and Jin, 2017; Dore et al., 2016; Stephens et al., 2018) have dramatically altered the forest disturbance regime once dominated by frequent, low-to-moderate intensity surface fires (Hagmann et al., 2021; North and Hurteau, 2011; Restaino et al., 2019; Stephens et al., 2007). Consequently, large areas of this region are covered by overstocked forests

* Corresponding author at: Wildlife Conservation Society (WCS), 2300 Southern Boulevard Bronx, New York 10460, USA.
E-mail address: evilanova@wcs.org (E. Vilanova).

https://doi.org/10.1016/j.foreco.2023.120945
Received 2 December 2022; Received in revised form 15 March 2023; Accepted 17 March 2023
Available online 4 April 2023
0378-1127/

that are often more vulnerable to drought, high-severity wildfires, increasing temperatures, and other disturbance agents (Stephens et al., 2018). A major worry under projected hotter and drier climate scenarios (Dettinger et al., 2018) is that critical ecosystem services (e.g., biodiversity, carbon storage, water regulation, and wildlife habitat) may be compromised by recurring wildfires burning at uncharacteristically high severity. For example, results from a recent study (Steel et al., 2022) justify this worry, where 30 % of the conifer forest extent in the southern Sierra Nevada transitioned to non-forest vegetation between 2011 and 2020 due to wildfires, drought, and drought-incited bark beetle epidemics.

A well-documented consequence of the structural changes produced by fire exclusion and suppression in forests across the western U.S., and particularly in California, is the substantial increase in fuel loads (Agee et al., 1977; Lydersen et al., 2019; Safford and Stevens, 2017; Steel et al., 2015). While ground and surface fuels provide important ecological functions (Harmon and Sexton, 1996), in combination with weather, topography and vegetation structure, these are also a fundamental driver of fire behavior and effects (Keane, 2013; Moritz et al., 2005). In the case of Sierra Nevada forests, greater surface fuel loads increase potential surface fire flame lengths leading to canopy torching and increased fire severity (Agee and Skinner, 2005; Stevens et al., 2017).

The significant departure from historical conditions that already existed in many Sierra Nevada forests, along with elevated rates of tree mortality broadly observed after the 2012–2016 drought (Axelson et al., 2019; Fettig et al., 2019; Robbins et al., 2022), increases the potential for ongoing and worsening hazardous surface fuel accumulations (Fig. 1). While the tree mortality episode that peaked in 2016 has slowed, as of

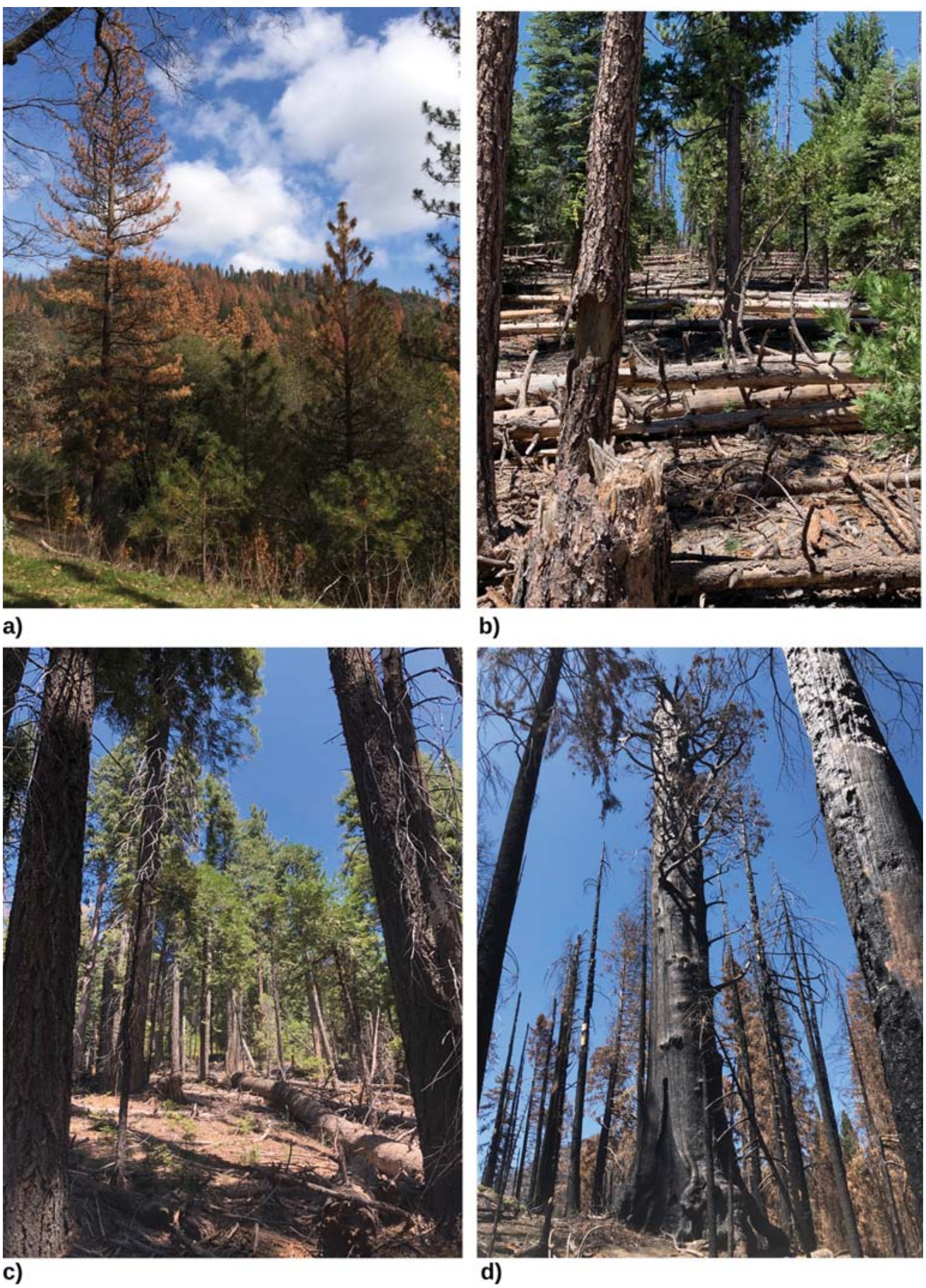

Fig. 1. Examples of high levels of tree mortality, high surface fuel loads, and severe wildfires effects in forests in the Sierra Nevada, California: a) Large numbers of dead trees after the drought near Goat Mountain, Sierra National Forest, 2017 (Photo credit: Christopher J. Fettig, Pacific Southwest Research Station, USDA Forest Service); b) High loads of large surface fuels near Bass Lake, Sierra National Forest, 2020 (Photo credit: Leif A. Mortenson, Pacific Southwest Research Station, USDA Forest Service); c) Dense forests and coarse woody debris at Yosemite National Park, California, 2020 (Photo credit: Emilio Vilanova, University of California); d) Large giant sequoia (*Sequoiadendron giganteum* (Lindl.) J. Buchholz) killed by the Castle Fire at the Mountain Home Demonstration Forest, California in 2020 (Photo credit: Emilio Vilanova).

2022 California continues in a multi-year drought (Williams et al., 2022) and tree mortality remains elevated in most areas (Wang et al., 2022), additional inputs to fuel biomass from current and future pulses of tree mortality are expected as tree health declines and snags (standing dead trees) breakdown and eventually fall to the forest floor. As such, robust characterization of wildland fuels has never been more important. On one hand, fuel reduction treatments are difficult to design and implement without an accurate quantitative description of fuels (Agee and Skinner, 2005; Cansler et al., 2019; Lydersen et al., 2014; Ryan et al., 2013). On the other, it is essential to document the immediate, post-disturbance conditions to understand the potential trajectory of future fuel conditions (Kennedy et al., 2021).

Because duff and surface fuels are essentially composed of dead biomass falling from the aboveground vegetation in different forms, sizes, and conditions, it is expected that forest composition and structure play a major role in their quantity and distribution. Yet, studies focusing on these relationships (e.g., Cansler et al., 2019; Collins et al., 2016; Lydersen et al., 2015) have shown mixed results with forest structure and composition being relatively weak predictors of surface fuel loads, ultimately reflecting the intricacy of accurately estimating surface fuel loads. The overarching goal of this study is to evaluate how well we can classify and predict post-disturbance fuel loads across a large geographic region. Here, we combined two networks of field measurements in the Sierra Nevada to produce the extensive, high-quality data needed to inform fire management applications (Keane 2013). For this, we used fuel measurements taken between 2016 and 2018 from sites across the Sierra Nevada to explore potential environmental and disturbance-related predictors of fuel loads. Specifically, we asked three main questions:

1) What is the magnitude and distribution of surface fuels after the 2012–2016 drought in the western Sierra Nevada, but **prior** to the commencement of widespread snag fall, across a range of forest conditions?
2) Can relatively distinct vegetation groups with different fuel load properties be identified to help streamline management approaches?
3) What combination of overstory metrics, biophysical factors and disturbance events best explain the amount and variability in duff and surface fuels across western Sierra Nevada forests?

A better understanding of fuel conditions following drought can help inform forest management, particularly given the growing attention to optimizing forest fuel reduction treatments to reduce wildfire risk, and the increasing frequency and extent of drought related tree mortality occurring under a warming climate. Ultimately, our results will not only help inform forest management in the Sierra Nevada, but also help evaluate the challenges for a learning-based approach (Gillson et al. 2019) to wildfire management in the era of global change.

2. Materials and methods

2.1. Study area

We combined two networks of permanent forest plots distributed across a latitudinal gradient in the western Sierra Nevada. Collectively, these 13 sites provide a broad sample of current conditions in Sierran mixed-conifer forests (Safford and Stevens, 2017). Prior to extensive fire suppression beginning in the early 20th century, these forests had low-to moderate severity frequent-fire regimes (i.e., < 35 years) (North et al., 2022; Safford and Stevens, 2017). They are dominated by a mix of tree species that may include ponderosa pine (*Pinus ponderosa* Douglas ex Lawson, PIPO), Douglas-fir (*Pseudotsuga menziesii* (Mirb.) Franco, PSME), incense cedar (*Calocedrus decurrens* (Torr.) Florin, CADE), white fir (*Abies concolor* (Gord. & Glend.) Lindl. ex Hildebr., ABCO), red fir (*Abies magnifica* A. Murray bis, ABMA), Jeffrey pine (*Pinus jeffreyi* Balf., PIJE), sugar pine (*Pinus lambertiana* Douglas, PILA), California black oak (*Quercus kelloggii* Newberry, QUKE), and giant sequoia (*Sequoiadendron giganteum* (Lindl.) J. Buchholz, SEGI) (Fig. A1-Appendix A). The climate of the western Sierra Nevada is Mediterranean with cool, wet winters followed by warm-to-hot, dry summers. Going forward, temperatures are expected to rise (3 to 5 °C on average by the end of the 21st century) and the summer drought period is expected to lengthen (Dettinger et al., 2018). Across the studies sites, normal (i.e., 1981–2010) annual precipitation is 830–1,270 mm, with higher values recorded in the northern Sierra Nevada (Fig. 2, Fig. A2-Appendix A). Of note, as much as a 40 % reduction in precipitation occurred during the 2012–2016 drought (PRISM Climate Group, 2020; Young et al., 2017) (Fig. 2). The warm and dry characteristics of this period, significantly enhanced by anthropogenic warming (Williams et al., 2020), were closely tied to a multi-year deep-rooting-zone drying influencing forest die-off (Goulden and Bales, 2019).

2.2. Field sampling and site description

Data collection occurred on a total of 462 plots. The majority (n = 282) were 12.62-m fixed-radius plots (plot area = 0.05 ha) installed between 2017 and 2018 as part of the California Tree Mortality Data Collection Network managed by University of California-Berkeley (UCB) (Axelson et al., 2019). Each of these sites were designed to capture landscape-level variations in forest conditions while not crossing major management, vegetation, or edaphic gradients. The UCB plot placement was stratified by generalized random tessellation sampling (GRTS) within each ~ 1.5–2.0 km^2 site (Stevens and Olsen, 2004).Thus, the final number of plots at each location ranged from 22 to 37, depending on terrain complexity (Table 1). The remaining plots (n = 180) are part of a network of 11.3-m fixed-radius plots (plot area = 0.041 ha) installed in 2016 and 2017 by the USDA Forest Service (USFS) at four sites, with 45 plots each in the Eldorado, Stanislaus, Sierra, and Sequoia National Forests. The USFS sampling approach design relied on a stratified random assignment of plots among latitudinal and elevational gradients. Moreover, sampling was concentrated in the more pine-dominated stands, where PIPO accounted for ≥ 35 % of total plot basal area (Fettig et al., 2019). Plots from both datasets occurred between 929 and 2,300 m in elevation (mean elevation = 1,605 m) (Table 1).

To document the disturbance history, we used data from different sources based on plot location. For past fire extents, we used the Fire and Resource Assessment Program (FRAP) database from the California Department of Forestry and Fire Protection (available at https://frap.fire.ca.gov/frap-projects/fire-perimeters/) that provides spatially explicit perimeters for fires > 4.05 ha in California. We included records of both wildfires and prescribed fires for 1950–2018. Information from the Monitoring Trends in Burn Severity program (MTBS, https://www.mtbs.gov/) which maps fire severity and extent of large fires (i.e., ≥ 404.7 ha) in the western U.S. from 1984–present was also used. The Rapid Assessment of Vegetation Condition after Wildfire (RAVG) program that produces data estimating post-fire vegetation conditions on National Forest System (NFS) lands was also examined for relevant information (https://burnseverity.cr.usgs.gov/products/ravg). Finally, we obtained data on timber harvests and hazardous fuel treatments for 1950–2018 from the Timber Harvest and Hazardous Fuels datasets from the USFS's Forest Activity Tracking System (FACTS) (https://data.fs.usda.gov/geodata/edw/datasets.php).

2.3. Plot data, over and understory measurements and fuel loads

In all 462 plots, a comprehensive set of metrics describing vegetation composition, forest structure, and fuel loading were collected. For trees ≥ 10 cm dbh, tree species, dbh, total height, and height to the base of the live crown were recorded. The condition of each tree was evaluated to determine its canopy stratum, status (i.e., live or dead, based on the presence or absence of live foliage), vigor class (live trees) or snag class (dead trees), and probable cause(s) of death. On USFS plots,

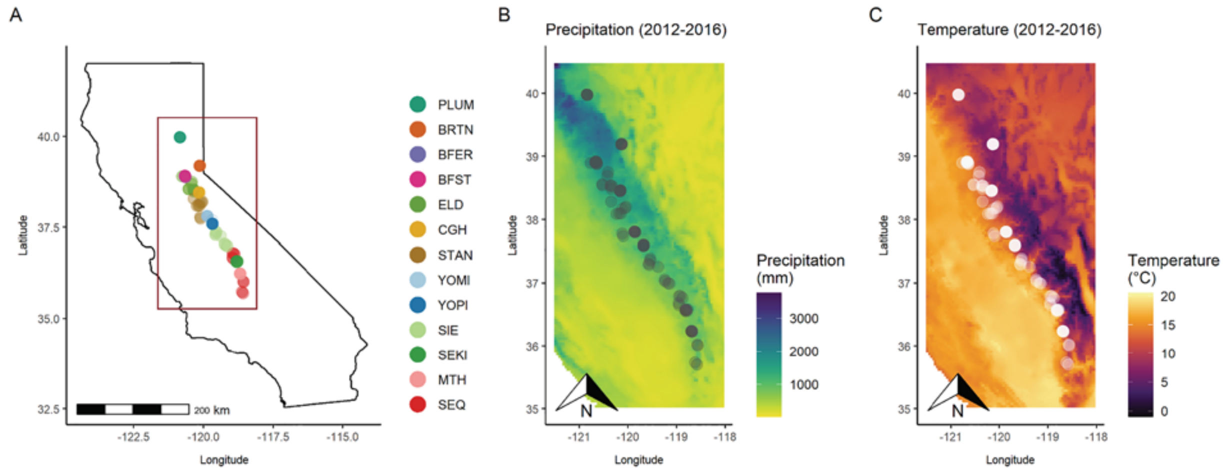

Fig. 2. A) Relative location of 462 plots over 13 sites in the Sierra Nevada, California. Shaded dots represent the approximate plot position including overlap within each location; B) Geographic location of plots over a map of mean annual precipitation (rainfall + snow) during drought period. Data from PRISM Climate Group (2020). C) Geographic location of plots over a map of mean annual temperature during the drought period. Data from PRISM Climate Group (2020). Location codes (N to S): PLUM: Plumas National Forest; BRTN: Burton Creek State Park; BFER: Blodgett Forest Research Station-Ecological Reserve; BFST: Blodgett Forest Research Station-Single Tree Selection; ELD: Eldorado National Forest; CGH: Cottonwood Gulch Watershed; STAN: Stanislaus National Forest; YOMI: Yosemite National Park-Mixed Conifer; YOPI: Yosemite National Park-Pine Dominated; SIE: Sierra National Forest; SEKI: Sequoia and Kings Canyon National Park; MTH: Mountain Home Demonstration State Forest; SEQ: Sequoia National Forest.

approximate year of tree death was also recorded (*see* Fettig et al., 2019). Combined, both datasets included information on 10,773 overstory trees, of which 66.2 % were alive at the time of our evaluations.

Fuel loads were measured in three transects per plot following the planar intersect method (Brown, 1974). In total, we measured fuel loads on 1,386 transects (mean of 106 transects per location). Fine woody debris (FWD) were classified by three diameter classes ($\leq$0.64 cm diameter; $> 0.64 \leq 2.54$ cm; $> 2.54 \leq 7.62$ cm) that correspond to 1-, 10-, and 100-hour fuel classes (Fosberg, 1970; Table A1, Appendix A). The FWD sample intensity, as defined by the transect length, differed slightly between the two plot networks. For the UCB plots, 1- and 10-h fuels were counted for 2 m and the 100-h fuels for 3 m. For the USFS plots, 1-and 10-h fuels were tallied for 1.8 m and 100-h fuels were tallied along 3.6 m. For both UCB and USFS plots, the diameter, species, and decay class were recorded for all 1000-h fuels (coarse woody debris; CWD with diameter > 7.62 cm) along the full length of each transect (12.61 and 11.3 m, respectively). Major and minor axis diameters were recorded for 1000-h fuels with oval or elliptical forms, and diameters were estimated for partially buried pieces. Finally, duff and litter depth were measured at one (USFS plots) or two (UCB plots) sampling points along each transect.

All duff and surface fuels were converted to equivalent estimates of biomass per unit area (Mg ha^{-1}). These estimations were done using the working version of the Rfuels package (Foster et al., 2018) which allows for rapid calculations of fuel loads, and includes all relevant equations developed for Sierra Nevada forests (van Wagdendonk et al., 1996; van Wagtendonk et al., 1998) widely used in related studies (e.g., Cansler et al., 2019; Collins et al., 2016; Lydersen et al., 2015; Stephens and Moghaddas, 2005). To ensure plot-level estimates captured differences in species composition, we used place-based loading corrections in which the coefficients required to calculate fuel loads were weighted by the relative basal area of the main constituent tree species in each plot.

2.4. Analytical approach

We took a tiered approach to our analysis of contemporary fuel loads across the Sierra Nevada. We started with a straightforward summary and comparison of site level differences (Question 1). Next, we applied clustering techniques to quantify the potential for overstory metrics (i.e., forest composition and structure) to identify consistent categories of fuel conditions (Question 2). Finally, we used a combination of variable importance analysis and mixed effects modeling to evaluate how well fuel loading can be predicted from a comprehensive array of overstory, biophysical, and disturbance variables (Question 3). This tiered approach builds in analytical complexity and incorporates results from earlier steps to inform subsequent steps.

To understand correlates of fuel loads across a range of forest conditions (Question 1), we summarized the mean and variance (i.e., 95 % confidence intervals) of the relevant structural, biophysical, and disturbance characteristics of each site (n = 13). Specifically, tree inventories were used to calculate the overstory tree structure by site. Plot-level biophysical factors included elevation, slope, aspect, and actual evapotranspiration (AET). AET (mm y^{-1}) for 1981–2010 was obtained from a 270-m resolution product from the California Basin Characterization Model (Flint et al., 2013, Table 1). AET has been shown to be well correlated with biomass production and can serve as a suitable proxy for the fuel loading in many ecotypes (Parks et al., 2014). The disturbance history was assessed using three metrics: type of disturbance (i.e., wildfire, prescribed fire, thinning or timber harvest), time since last disturbance, and number of disturbances recorded at each plot during 1950–2018. For each site, fuel loads were summarized by fuel class. Given the non-normal distribution of fuel data (Fig. A3-Appendix A), differences among sites were evaluated with the nonparametric Kruskal-Wallis test.

To determine if fuel loads were associated with overstory composition and structure (Question 2), we used the tree inventories to identify distinct vegetation groups. Groups were defined using *k-means* clustering, an unsupervised machine learning algorithm that groups similar plots together in order to discover underlying patterns (Gotelli and Ellison, 2004). To determine the optimal number of clusters in the data, we used the *gap statistic method* (factoextra R package, Alboukadel and Mundt, 2020) and selected the number of clusters that maximized this value (Tibshirani et al., 2001). After determining the number of clusters, we used the *kmeans* function to conduct the clustering of vegetation groups with a maximum of 250 iterations (4.2.2 version of the R software, R Core Team, 2022). Since there are more than two dimensions (i.e., variables) being used, one of the results of this analysis is a Principal Component Analysis (PCA) including plots within vegetation clusters. All predictor variables were relativized by range to account for different units and dimensions. Following the clustering analysis, we summarized

Table 1

General description of study sites. AET: Actual evapotranspiration for 1981–2010 obtained from a 270-m resolution product from the California Basin Characterization Model for California (Flint et al., 2013). QMD: Mean plot quadratic mean diameter. CI: 95 % confidence intervals. SD: Standard deviation. UCB: University of California-Berkeley; USFS: USDA Forest Service. Sites organized approximately from north to south. [1] Mean of years since a disturbance event (i.e., thinning, timber harvest, wildfire or prescribed fire) was recorded at each plot during 1950–2018.

Jurisdiction / ownership	Location name	Location code	Data source	Number of plots	Mean elevation (m)	Mean AET (mm y^{-1})	Mean QMD (cm)	Live basal area (m^2 ha^{-1})		Live tree density (trees ha^{-1})		Dead basal area (m^2 ha^{-1})		Dead tree density (trees ha^{-1})		Mean time since last disturbance (years)
								Mean	**95 % CI**	**Mean**	**95 % CI**	**Mean**	**95 % CI**	**Mean**	**95 % CI**	
National Forest	Plumas	PLUM	UCB	29	1,479	408.9	28.9	51.2	7.5	855.2	132.4	4.6	2.1	52.4	25.7	28
State Park	Burton Creek	BRTN	UCB	36	2,026	361.3	46.2	49.6	7.1	349.4	83.9	10.3	3.8	63.3	26.9	60.5
Research Forest	Blodgett Forest-Ecological Reserve	BFER	UCB	22	1,307	577.9	55.6	117.4	21.0	481.8	75.3	18.2	11.5	127.3	34.1	68
Research Forest	Blodgett Forest-Single Tree Selection	BFST	UCB	22	1,308	585.2	44.4	68.2	8.1	462.7	56.6	4.9	2.2	55.5	16.7	14.3
National Forest	Eldorado	ELD	USFS	45	1,369	505.2	35.9	23.2	6.1	254.4	60.6	40.6	7.1	213.9	32.6	54.1
National Forest	Cottonwood Gulch Watershed	CGH	UCB	36	2,168	381.1	45.9	62.1	11.3	387.8	68.0	12.6	5.9	58.3	16.5	17.4
National Forest	Stanislaus	STAN	USFS	45	1,323	483.8	32.9	15.6	4.0	197.2	48.8	42.9	7.0	277.8	48.4	20.1
National Park	Yosemite-Mixed Conifer	YOMI	UCB	37	1,420	446.1	60.7	62.4	15.7	216.8	37.0	49.8	12.3	222.7	40.5	5.2
National Park	Yosemite-Pine	YOPI	UCB	35	1,719	380.6	38.7	44.4	14.4	366.3	67.9	43.5	13.1	261.1	71.1	64.5
National Forest	Sierra	SIE	USFS	45	1,398	456.1	29.1	9.7	3.0	190.6	52.4	43.6	6.2	297.8	41.0	48.9
National Park	Sequoia and Kings Canyon	SEKI	UCB	29	1,694	374.7	43.9	46.5	10.5	322.8	66.2	38.9	8.0	180.7	52.7	50.2
State Demonstration Forest	Mountain Home	MTH	UCB	36	1,944	356.1	76.9	124.4	40.3	253.3	36.7	37.7	21.0	82.8	24.9	68
National Forest	Sequoia	SEQ	USFS	45	1,716	353.7	31.9	15.3	3.5	228.9	51.1	38.9	6.4	250.6	33.6	38.4
			Mean	36	1,605	436.2	43.9	53.1	11.7	351.3	64.4	29.7	8.2	164.9	35.7	41.2
			Std. Dev.	8	295.4	81.3	13.9	35.8	10.1	179.7	24.7	16.7	5.2	94.6	15.3	28.1

forest characteristics and surface fuel loads for each of the clusters identified. For these analyses, we simplified the fuel classes into three groups: FWD + litter, duff, and 1000-h fuels to reflect their combustion behavior. Litter and FWD dry quickly, making them readily available to burn, thus are the primary fuel for wildfire ignition and spread (Goodwin et al., 2021). In contrast, the duff layer is consumed by smoldering combustion in the wake of the flaming front and may produce heat for a much longer duration. Fire can also persist in the heavy woody fuel (i.e., 1000-h fuel) and generate heat for prolonged periods due to the dampening effect of their moisture content (Goodwin et al., 2021; Knapp et al., 2005). Here, we again used the Kruskal-Wallis statistic to test for differences in fuel loads among clusters.

We evaluated the skill of potential predictors of duff and surface fuels (Question 3) through a series of analyses designed to build generalized mixed effects models that best explain the data while also protecting against overfitting (i.e., an information theoretic approach, Burnham and Anderson, 2002). First, we documented correlations among variables and fuel loads by producing a pair-wise Kendall's tau (τ) correlation matrix. Given the abundance of correlations among potential predictions, we applied a random forest analysis to rank the most important variables (function *varImp* in the caret R package; Khun, 2020) in terms of their ability to predict each response (i.e., duff, FWD + litter, and 1000-h fuels).

Prior to analysis, aspect was transformed to account for the circular nature of the measure (Martinez et al., 2019), and then all continuous variables were centered and standardized to directly compare their effects. The results from the variable importance analyses informed the development of generalized mixed effects models for the three major classes of fuels. The top five variables in importance were initially used to test alternative models for each fuel class. Based on the significance of each predictor, a stepwise selection process was followed to sequentially eliminate variables from the original full (saturated) model to find a reduced version that best explained each fuel class. If a high degree of collinearity was detected between variables that were ranked as most important (e.g., SDI and QMD), we added the next most important independent variable. A component of plot within location was included as a random effect in all the models tested, while all explanatory variables were fixed effects. The amount of variation explained by random and fixed effects was quantified by calculating the conditional (c) and marginal (m) R^2 for all models. R^2c is indicative of the variance explained by both fixed and random effects, whereas R^2m indicates the variance explained by fixed effects only (predictive variables) (Nakagawa and Schielzeth, 2013). The 'best' model was selected based on the corrected version of the Akaike information criterion (AICc) (Johnson and Omland, 2004). The mixed effects models were built using the glmmTMB R package (Brooks et al., 2017). R^2 and *AICc* values were calculated using the MuMIn R package (Barton, 2022).

3. Results

3.1. Fuel loadings across sites

Throughout the study area, fuel loads tended to be high, with an average sum for all fuel classes of 138.2 ± 21.7 (mean ± 95 % CI) Mg ha^{-1}. On average, 44 % of the total fuel loadings was composed by CWDs, followed by duff (28 %), litter (22 %) and FWD (6 %). However,

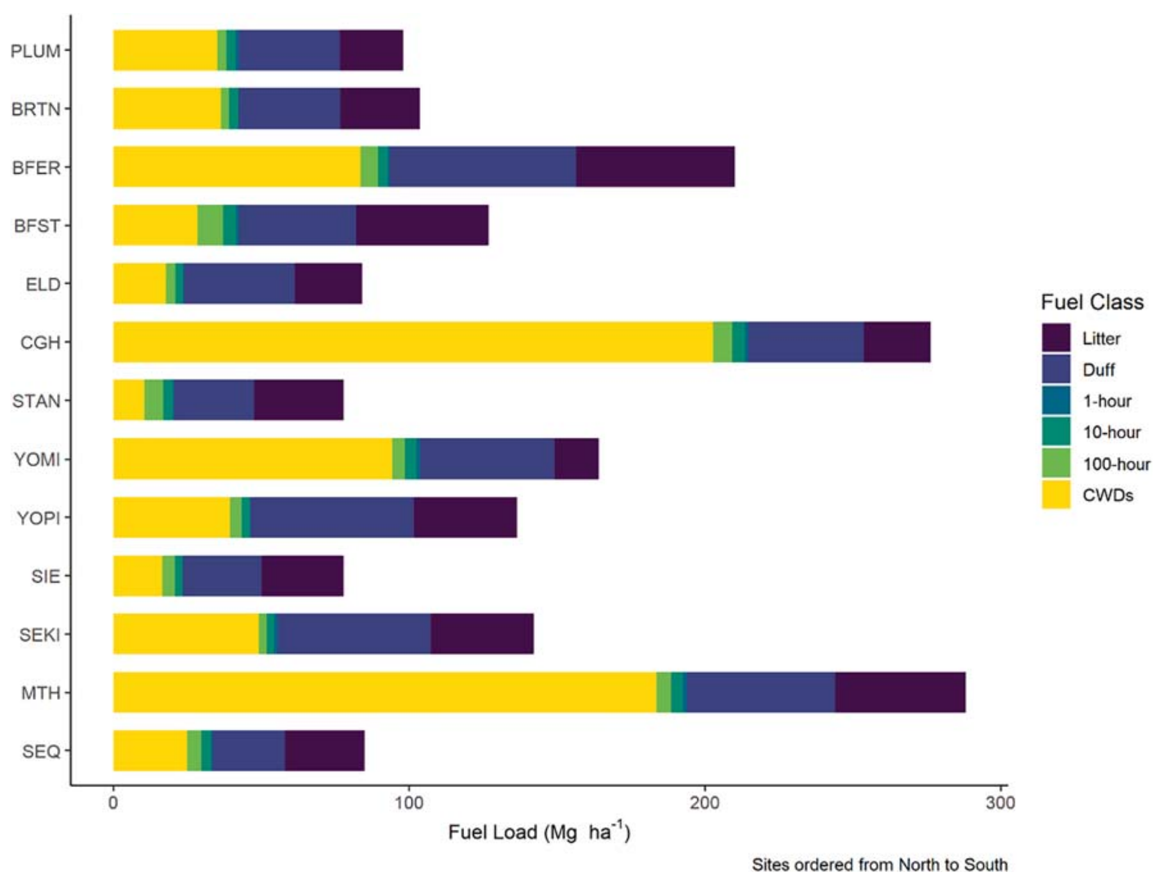

Fig. 3. Mean duff and surface fuel loads for 13 sites in the western Sierra Nevada, California. Site codes (from north to south): PLUM: Plumas National Forest; BRTN: Burton Creek State Park; BFER: Blodgett Forest Research Station-Ecological Reserve; BFST: Blodgett Forest Research Station-Single Tree Selection; ELD: Eldorado National Forest; CGH: Cottonwood Gulch Watershed; STAN: Stanislaus National Forest; YOMI: Yosemite National Park-Mixed Conifer; YOPI: Yosemite National Park-Pine Dominated; SIE: Sierra National Forest; SEKI: Sequoia and Kings Canyon National Park; MTH: Mountain Home Demonstration State Forest; SEQ: Sequoia National Forest.

there was large variation in surface fuels across and within sites (Fig. 3; Table B1-Appendix B). The greatest variation was found for the 1000-h class with a mean of 60.9 ± 20.8 Mg ha^{-1} (range of 0–3,627.9 Mg ha^{-1}). Within FWD, a mean of 0.7 ± 0.1, 3.2 ± 0.2, and 4.6 ± 0.5 Mg ha^{-1} was estimated for 1-, 10- and 100-h fuels, respectively. Litter accounted for 29.8 ± 1.7 Mg ha^{-1} on average, with duff being 39.0 ± 2.4 Mg ha^{-1}. We found significant differences across all 13 sites and for every fuel class (Table B1; Fig. B1-Appendix B). The highest biomass for litter (53.8 ± 14.8 Mg ha^{-1}) and duff (63.0 ± 9.9 Mg ha^{-1}) was found at BFER. CGH had the highest biomass for 1-h (1.3 ± 0.3 Mg ha^{-1}), 10-h (4.3 ± 0.9 Mg ha^{-1}), and 1000-h fuels (202.7 ± 144.9 Mg ha^{-1}). The highest biomass for 100-h fuels occurred at BFST (8.7 ± 1.9 Mg ha^{-1}). At both CGH and MTH we found the highest maximum values for 1000-h fuels, largely influenced by the presence of several large logs in a few plots at both sites (Fig. 3; Fig. B1-Appendix B).

3.2. Vegetation clustering

The *k-means* analysis resulted in four distinct vegetation clusters based on the tree inventory data (Fig. 4; Fig. B3-Appendix B). Three major dimensions (i.e., axes) explained close to 50 % of the variation in the overstory composition and structure with basal area (live and dead), tree density (live and dead), SDI, and QMD being the most relevant variables. Two related compositional variables, proportion of PIPO and SEGI, also appeared as major contributors for the overall distribution of plots in this multivariate space. Contribution of the remaining axes was relatively low reaching a combined total 80 % of the variance threshold with nine dimensions (Fig. B4-Appendix B). The first vegetation cluster (i.e., cluster 1) was composed of 108 plots located in areas dominated by three species CADE, PSME, and PIPO, and also characterized by the highest density of live trees and the lowest basal area of dead trees among the four clusters. The second vegetation cluster grouped 117 plots mostly dominated by ABCO, ABMA, PILA, and to a lesser extent by PIPO, and was characterized by the second highest density of live trees. The third vegetation cluster is perhaps the most distinct, with only 14 plots dominated by SEGI and the highest live basal area among all clusters. Finally, the largest vegetation cluster grouped 223 plots and was dominated by PIPO, CADE, and to a lesser extent by QUKE. This group was characterized by the highest density of dead trees, the lowest SDI and lowest live basal area among all clusters (Table 2; Fig. B5-Appendix B).

Overall, these clusters seem to fit well into two major axes: 1) one mostly linked to live basal area where large SEGI trees (Cluster 3) dominate, and 2) a mortality axis representing a gradient from PIPO stands with high tree mortality and low tree density to PSME and CADE stands with higher densities of live trees. Finally, we found significant differences in fuel loads among all clusters (Fig. 5). The SEGI-dominated group (cluster 3) was characterized by the highest values for all fuel classes combined (mean = 547.6 Mg ha^{-1}), for which 1000-h fuels accounted for nearly 77 % of the total. On the other hand, the PIPO-dominated group (cluster 4) had the lowest values for all fuel classes (mean = 90.1 Mg ha^{-1}) (Fig. 5).

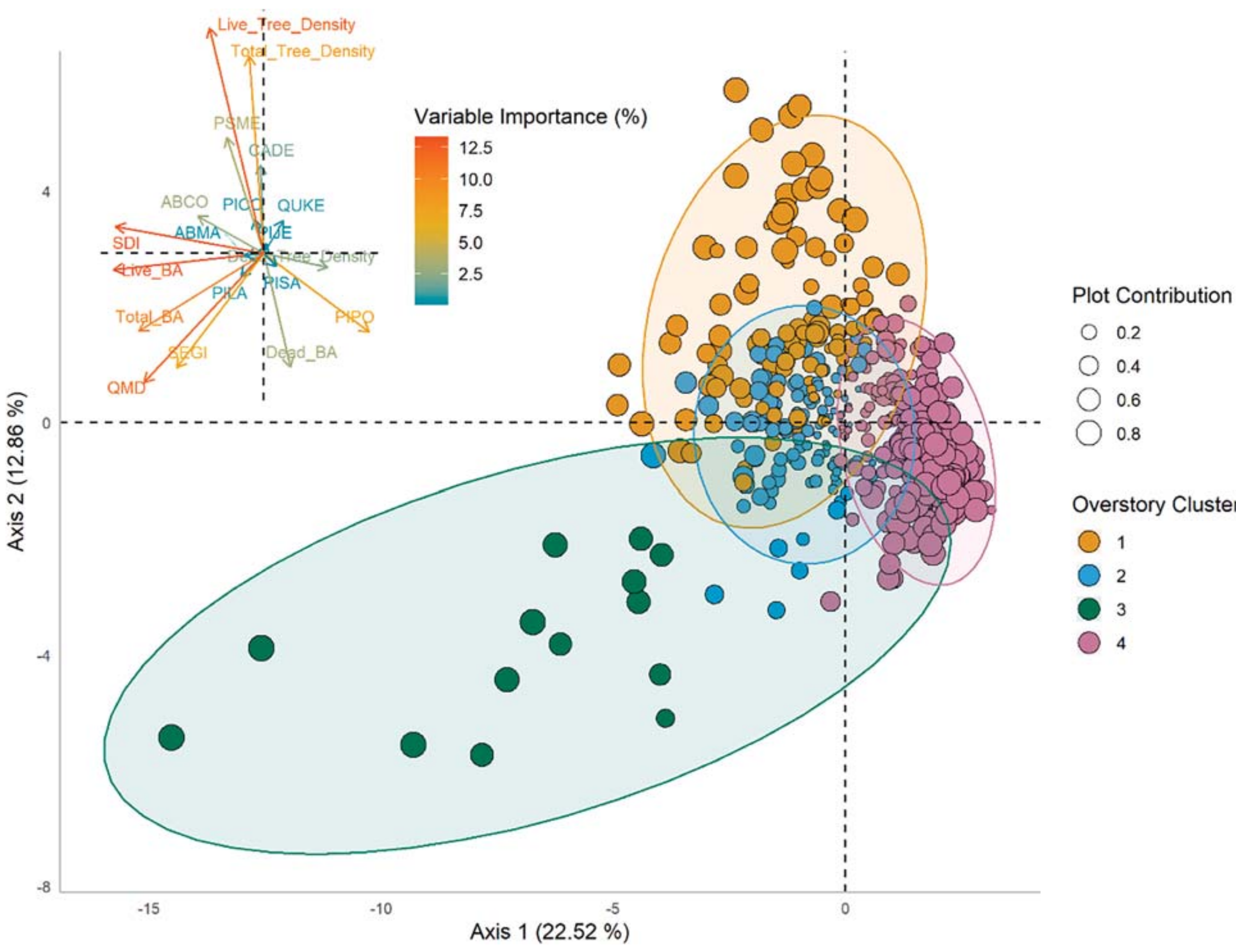

Fig. 4. Principal Component Analysis (PCA) output from the *k-means* clustering indicating four major vegetation groups based on overstory structure and composition. Inset shows the direction and relative importance of all variables. Main characteristics of the clusters shown in Table 2. For a detailed description of the variables used in this analysis see Table B2 and Figures B5-B6-Appendix B.

Table 2
Main environmental and structural characteristics of the four vegetation clusters identified. For elevation and AET, values are mean ± standard deviation; for basal area and density, values are mean ± 95 % confidence intervals. Based on live tree basal area, clusters were aligned with vegetation alliances defined by the US Forest Service Vegetation and Classification in California system (CalVeg) (USFS, 2009).

Cluster	Elevation (meters)	AET (mm year^{-1})	Live basal area (m^2 ha^{-1})	Dead basal area (m^2 ha^{-1})	Density of live trees (trees ha^{-1})	Density of dead trees (trees ha^{-1})	Dominant tree species (% of live basal area)
1	1503 ± 224	468.6 ± 91.5	80.8 ± 8.1	17.4 ± 3.9	618.1 ± 55.1	134.4 ± 23.5	Incense cedar (30.3 %), Douglas-fir (19.9 %) and Ponderosa pine (18.4 %). Alliance: Mixed Conifer-Pine.
2	1900 ± 280	386.7 ± 64.7	55.1 ± 5.4	21.5 ± 5.6	291.2 ± 27.1	90.3 ± 17.4	White fir (46.1 %), Red fir (13.9 %), Sugar pine (20 %) and Ponderosa pine (3 %). Alliance: Mixed Conifer – Fir.
3	1960 ± 44.7	356.9 ± 22.7	232.1 ± 71.8	55.4 ± 46.4	231.4 ± 43.2	60 ± 31.3	Giant sequoia (68.3 %), White fir (19.6 %) and Sugar pine (10.1 %). Alliance: Big Tree.
4	1488 ± 264	438.4 ± 80.4	16.7 ± 1.9	43.1 ± 3.6	208.9 ± 20.7	252.9 ± 20.3	Ponderosa pine (66.6 %), Incense cedar (16.6 %), and California black oak (7.7 %). Alliance: Ponderosa Pine.

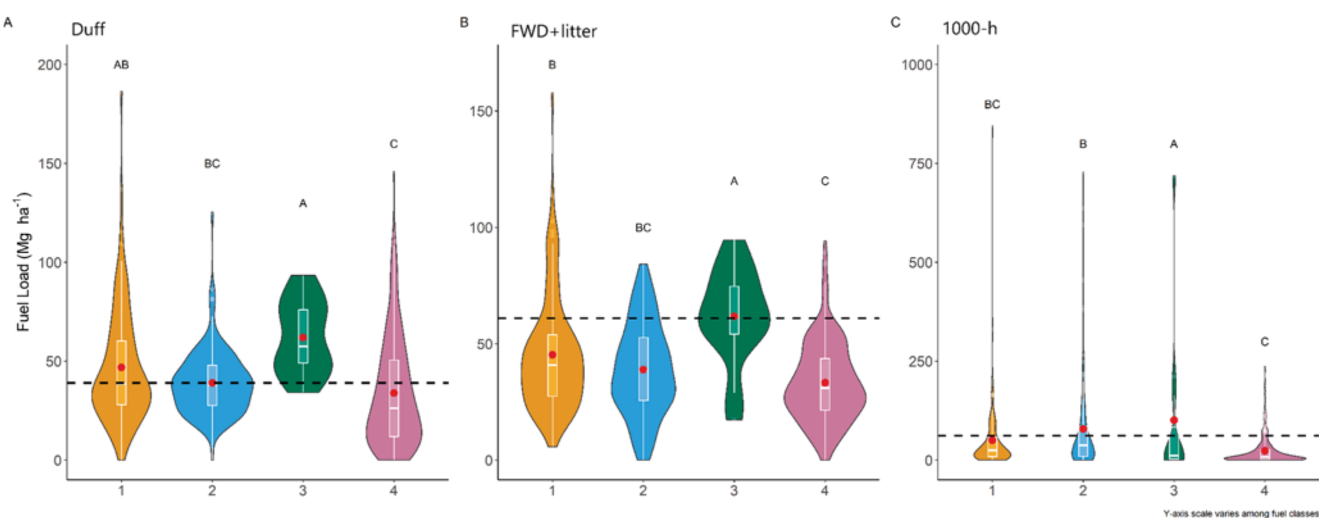

Fig. 5. Violin plots for three major fuel classes across four vegetation clusters in western Sierra Nevada forests: A) Duff layer; B) FWDs + Litter; C) CWDs (1000-h fuels). For visualization Y-axis has been limited to 1,000 Mg ha^{-1}. White box plots within violin plots show median (white bar), interquartile range (25 % quartile and 75 % quantile; white box), 95 % confidence intervals (white lines within colored areas). Red dots represent the mean for each cluster. Black dashed lines show the overall mean value for each fuel class. Significant differences ($P < 0.001$) were found in all cases based on a Kruskall-Wallis non-parametric test with a posthoc to define possible groups. Width of violin plots is based on the probability density (colored shaded areas) for the range of observations (y-axis). Diameter classes of woody fuels are: ≤ 0.64 cm diameter (1-h); > 0.64 ≤ 2.54 cm (10-h); > 2.54 ≤ 7.62 cm (100-h), > 7.62 cm (1000-h). Cluster (C)1: 108 plots; C2: 117 plots; C3: 14 plots; C4: 223 plots.

3.3. Potential predictors of fuel loads in Sierra Nevada forests

3.3.1. General correlations among variables and fuel loads

In general, relatively low ($\tau < 0.3$) correlations between fuel loads and overstory metrics were common across all fuel classes (Fig. B7-Appendix B). Total and live basal area, as well as density of live trees had low but significant and positive correlations with duff, litter, and FWD. SDI, live basal area, and QMD all had positive and significant correlations with 1000-h fuels. Among the biophysical parameters tested, aspect also had weak but significant and positive correlations with fuel loads. Surprisingly, time since the last disturbance event or the number of these events were found to have very weak relationships with all overstory variables and fuel classes. The highest correlation τ values were ~ 0.1 on average and were only significant for density of live trees among the overstory variables, and for duff and litter among fuel classes (Fig. B7 Appendix B).

3.3.2. Variable importance

Results of the assessment of variable importance using a random forest algorithm identified potential predictors of surface fuel loads that varied in their composition and explanatory power for each fuel class. For duff, total basal area and other structural-based variables, such as SDI or the density of live and dead trees, were ranked as most important, while most, if not all, the biophysical-related variables had a lower ranking (15–18 % in variable importance; Fig. 6A). For FWD + litter, AET (29.6 %), in combination with total and live basal area (23.9 %), time since last disturbance (20.5 %) and elevation (20.3 %) were the top-five most important variables for this fuel class (Fig. 6B). In general, the potential predictors for 1000-h fuels explained little of the measured variation (6.1 %). Aspect, density of live trees, slope, total basal area, and dead tree basal area were the top-five ranked variables for 1000-h fuels (Fig. 6C).

3.3.3. Mixed effects modelling

To further evaluate potential predictors of fuels, we tested two different models for each of the three fuel classes for a total of six models, and identified the best model as the one with lowest AICc score. For comparison, we included the best fit model (i.e., highest R^2m). Note: since only continuous variables were ranked high in terms of variable importance, we centered and standardized these variables to be able to directly compare their effect size in the model. For duff, the model with the lowest AICc included SDI and the density of dead trees with SDI having a larger positive effect on duff mass than dead tree density. However, its low R^2m (0.21) indicates that it explained a relatively small amount of the variation present, especially in comparison to the best fit model that included the same variables plus total basal area (Fig. 7;

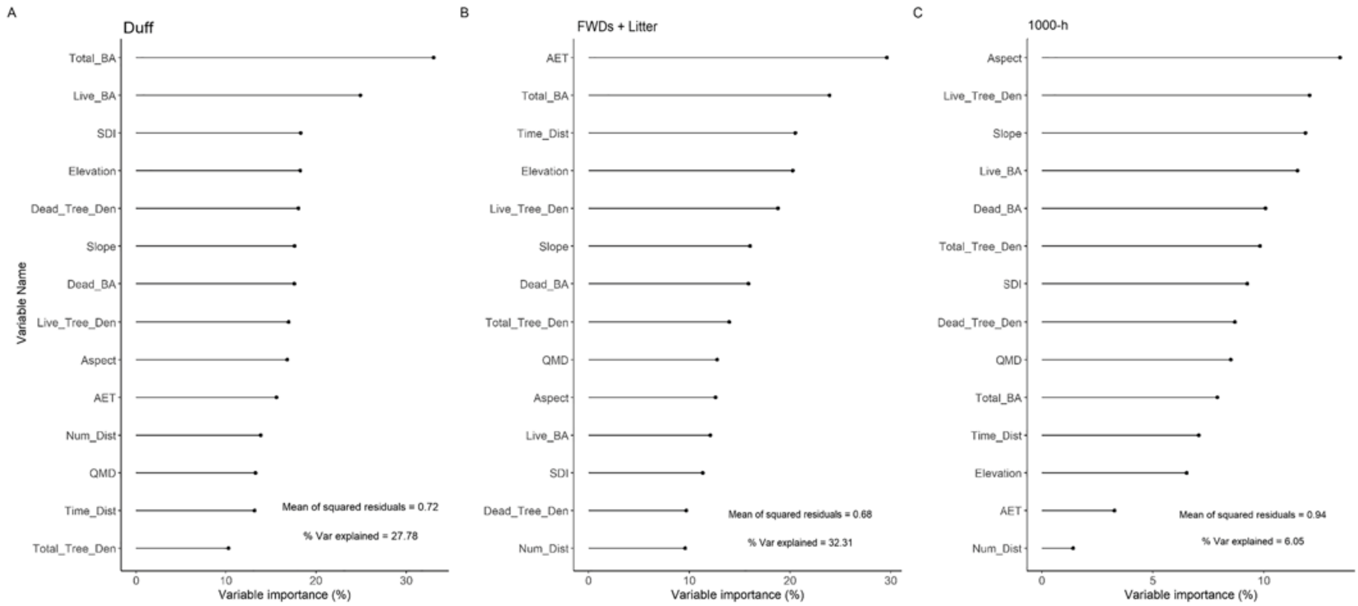

Fig. 6. Analysis of variable importance (VIMP) for three fuel classes in 462 forest plots in the Sierra Nevada, California. A) VIMP for duff (Variance explained = 27.8 %); B) VIMP for FWDs + Litter (Variance explained = 32.3 %); C) VIMP for 1000-h fuels (CWDs) (Variance explained = 6.1 %).

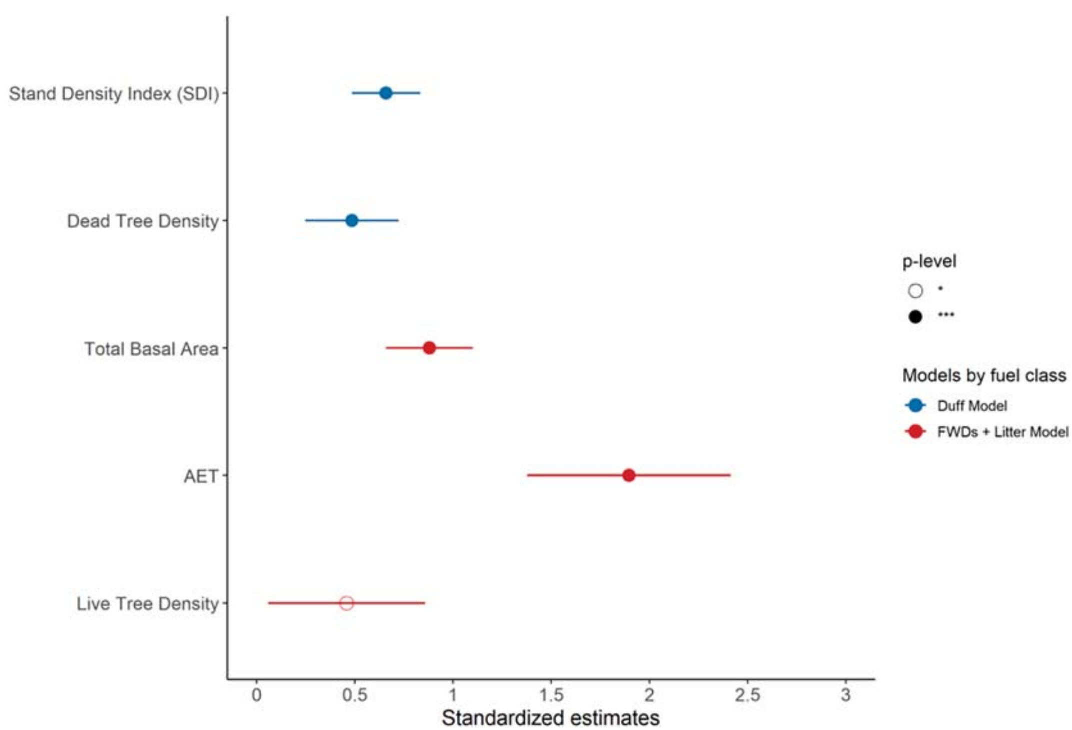

Fig. 7. Standardized estimates (effect size) for selected models of duff (blue symbols) and FWD + Litter (red symbols). Duff Model: Duff ~ SDI + Dead_Tree_Den + (1|Plot:Location); FWDs + Litter Model: FWDs_Litter ~ Total_BA + AET + Live_Tree_Den + (1|Plot:Location). Model for CWDs not shown. Each variable shows the standardized coefficients with 95 % confidence intervals. Significant values are indicated with open (*$P < 0.05$) and closed circles (***$P < 0.001$). Details of each model are shown in Tables B4-B6 in Appendix B.

Table B4-Appendix B).

For FWD + Litter, we found that both models were similar and with a high R^2m (>0.81). The most parsimonious model included AET, total basal area (live and dead), and density of live trees (Fig. 7, Table B5-Appendix B). All variables had a positive effect on FWD + Litter mass with AET being the most influential. For CWD, both models had an overall low performance with the combination of live basal area and the density of live trees explaining only ~ 11 % of the variance for this fuel class (R^2m = 0.11) (Table B5-Appendix B).

4. Discussion

High levels of surface fuel biomass were found at most sites across our extensive network of field plots in Sierra Nevada mixed-conifer forests (Fig. 2; Table B1-Appendix B). Compared to other estimates of fuel loads before and after fuel reduction treatments or wildfires, our values tend to be closer to pre-disturbance levels (e.g., Collins et al., 2016; Stephens et al., 2012; Vaillant et al., 2009) reflecting that most plots in our study were lacking recent disturbance altering ground and surface fuel biomass. Indeed, nearly half of the plots showed no record of disturbance between 1950 and 2018 (Table 1, Table B3, Fig. B8-Appendix B). Importantly, the average total fuel load across our plot network (138.2 Mg ha^{-1}) may be up to five times higher than during the pre-fire exclusion era (circa 1800) for mixed-conifer forests in California (i.e., mean = 26.9 Mg ha^{-1}, Stephens et al., 2007). Other relevant works report average total duff + surface fuel loads of 91–212 Mg ha^{-1} in unburned areas and 3–60 Mg ha^{-1} one year after fire (Cansler et al., 2019; Knapp et al., 2005).

Measurements for individual fuel classes were also comparable to those reported elsewhere. For instance, the average biomass of duff (39.9 Mg ha^{-1}) and litter (31.2 Mg ha^{-1}) in our study is in the range of values observed in other relevant studies (30–72 Mg ha^{-1} for duff and 12–34 Mg ha^{-1} for litter; Knapp et al., 2005; Lydersen et al., 2019, 2015; Van de Water and North, 2011). Similarly, fine fuels (1-, 10- and 100-h fuels) averaged 8.53 Mg ha^{-1}, which approximates estimates of mean fine fuels in the Lake Tahoe Basin, California (range = 4.4–12.9 Mg ha^{-1}; Taylor et al., 2014), but the maximum value observed in our study was much higher (62.8 Mg ha^{-1}). Estimates of CWD (1000-h fuels) averaged 63.3 Mg ha^{-1}, a value generally higher than those from previous studies (e.g., Low et al., 2021; Lydersen et al., 2015; Lydersen and North, 2012). The higher values in this study may be due to the greater variety of forest conditions included, particularly those sites with greater abundance of ABMA and SEGI that tended to have the largest CWD loads (i.e., CGH and MTH; Fig. 3). A large range and long right-tailed distribution, as observed in our study, is typical of 1000-h fuels. For example, Lydersen et al. (2019) found a range of 0–1,101 Mg ha^{-1} among plots in the Kings River Experimental Watershed in the southern Sierra Nevada prior to prescribed fire. We found a range of 0–3,628 Mg ha^{-1} among plots. CWD among sites tends to vary with the presence of large trees, with lower loads existing in areas with a history of timber harvest (Cansler et al., 2019).

With the exception of duff and litter (for which our estimates were lower), both of our sites in Yosemite National Park (YOMI and YOPI) showed very similar values to the pre-2013 Rim Fire fuels estimates reported by Cansler et al. (2019) in the Yosemite Forest Dynamics Plot (YFDP). One possibility for the observed differences in duff and litter between our studies is the higher abundance of very large trees (dbh > 60 cm) at YFDP. A consistent result from our analyses was the positive correlation between total basal area and duff biomass. Given the contribution of large trees to total basal area (i.e., increases as the square of tree diameter), the results from the YFDP match these expectations. The accumulation of duff and litter around the base of large conifers is an important source of fuel heterogeneity in western forests (Lutz et al., 2020; Ryan and Frandsen, 1991). Furthermore, higher duff loads can occur in long-unburned forests and when subjected to fire can burn as a smoldering fuel, exposing underlying mineral soil, roots, and nearby stems to long-duration heating (Banwell and Varner, 2014; Frandsen, 1987). When fires burn in these fire-excluded stands, smoldering around these deep basal accumulations can result in substantial mortality of codominant and dominant trees (Stephens and Finney, 2002).

In aggregate, the overstory characteristics of Sierran forests explained 80 % of the observed variation in fuel loads. Moreover, this variation was parsed into four vegetation clusters (Fig. 4) from which significant differences in fuel loads were detected (Fig. 5). However, it was the ‘extremes’ in fuel loads that drove the primary gradient in the clustering analysis. On the high end, SEGI-dominated stands (cluster 3) which attained up to 124.4 m^2 ha^{-1} of basal area (Table 1) supported the largest fuel loads (Fig. 5, median = 147 Mg ha^{-1}). On the low end, PIPO-dominated stands where there were more standing snags than live trees (cluster 4) contained the lowest fuel loads (Fig. 5, median = 78 Mg ha^{-1}). For the clusters with intermediate estimates of fuels (i.e., clusters 1 and 2), our analyses did not reveal significant differences in fuel loads (Fig. 5). These two groups also had the highest tree density, with particularly high density in the lower elevation CADE/PSME/PIPO group (cluster 1) compared to the higher elevation ABCO/ABMA/PILA group (cluster 2) (Table 2).

These four clusters broadly align with the vegetation alliances used by the USDA Forest Service in California (USFS, 2009) (Table 2). Thus, insights from this analysis can inform management more generally across the region. For example, there are few comparable studies for the Big Tree alliance (SEGI-dominated cluster 3). One exception is Weise et al. (1997) who combined photo series and field transects and reported 7–170 Mg ha^{-1} in total fuel loads for several SEGI groves. We generally found higher fuel loads in our SEGI dominated plots with the 1000-h fuel class as the largest contributor (Fig. 5). For example, at Mountain Home Demonstration State Forest (MTH), fuel loads ranged from 30.3 to 3,800.3 Mg ha^{-1} with an average of 288.1 Mg ha^{-1}. This difference could reflect site differences or possibly additional accumulation of fuels over the 20 + years between our study and Weise et al. (1997). A better understanding of fuel loads in SEGI-dominated forests is a high priority given the recent fire impacts to some SEGI groves (Shive et al., 2022; Fig. 1D). In addition, the similarity in fuel loads (Fig. 5) between the Mixed Conifer-Pine (cluster 1) and Mixed Conifer-Fir (cluster 2) suggests that, to some extent, management strategies for addressing ground and surface fuel loads in these alliances could be similar, at least in areas that generally lack recent disturbance.

While fuel loading was lowest (Fig. 5) in the Ponderosa Pine alliance (cluster 4), much of the tree mortality that occurred during the recent mortality event was concentrated in this group and attributed to colonization of PIPO by western pine beetle (*Dendroctonus brevicomis* LeConte) in 2015 and 2016 (Fettig et al., 2019). Under these conditions, we thus should expect significant increases in surface fuels in the near future. On one hand, FWD and litter can be significantly driven by canopy cover in PIPO-dominated stands (Hall et al., 2006), so with a decline in forest health with decaying and dead trees, an important influx of these small fuels might be expected. On the other hand, these snags were mostly still standing at the time of our evaluations and thus had not yet contributed much to the 1000-h fuel class. However, with the relatively faster rate of snag fall reported for PIPO, with a median of 6 years (Raphael and Morrison, 1987), in comparison to other species such as CADE with median fall rates up to 11 years (Grayson et al., 2019), particularly 1000-h fuels are expected to increase in the next several years as these snags fall to the forest floor. This projected increase in 1000-h fuels, coupled with the already high surface fuel loads, needs to be considered in any risk analysis, especially with recent evidence of large and severe fires driving important changes in Sierra Nevada mixed-conifer forests (Cova et al., 2023; Steel et al., 2022).

Our ability to model duff and surface fuel loads from overstory metrics, biophysical variables, and disturbance history varied greatly by specific fuel class (Figs. 6–7). For the fine fuels (litter + FWD), three commonly available variables (AET, total basal area, and live tree density) explained 81 % of the variation (Table B4). In contrast, we had no skill in predicting 1000-h fuel loads (Table B5) and only weak ability to estimate duff loads (Table B3). The amount of variation explained by our fine litter model stands out in comparison to other attempts to model surface loads in comparable Sierran forests (Cansler et al., 2019; Collins et al., 2016; Lydersen et al., 2015). The model with the best fit from these three studies had a R^2 = 0.31 (Collins et al., 2016). However, in terms of duff and 1000-h fuel classes, our results (weak to none) were no better at identifying the variables that shape fuel dynamics in these forests.

Wildland fuelbeds consist of diverse particles of many sizes, types, and shapes with abundances and properties that are highly variable (Keane, 2013). Thus, linear sampling methods (i.e., transects) may not efficiently capture the spatial variability that characterize surface fuels (Keane and Gray, 2013), particularly for 1000-h fuels. In addition, the distribution of wildland fuels tends to be clumped at multiple spatial scales and the loads tend to be heavily right tailed (e.g., Fig. 5; Fig. B1;

Prichard et al., 2019). In fact, while the effects of the overall lack of disturbance events might partly explain our high estimates of surface fuels, associated variables (i.e., time since last disturbance and number of disturbance events) were not selected as predictors in any of our final models. Thus, accurately estimating fuels loads, particularly for heavy fuels, is challenging emphasizing the need for a better understanding of the spatial dimensionality when characterizing fuels (Prichard et al., 2022). More data, whether obtained by increasing the field sampling intensity (i.e., longer fuel transects and large sample sizes), and/or deploying new technologies (e.g., remotely sensing) are needed to capture the full range of variation of fuels on these landscapes.

Perhaps not surprisingly, the clearest relationships in most of our sites is that heavily stocked forests with more trees (i.e., higher basal area) and with less disturbance tend to have higher surface fuel loads (Fig. 7; Fig. B7-Appendix B). While we expected dead trees to be a good predictor of surface fuel loads, in fact the live overstory tree component was a better predictor. In addition, AET, a proxy for forest productivity (Parks et al., 2014), proved to be an important predictor of litter and FWD (Fig. 7). The apparent decline in fuel load with increasing tree mortality, at least at the time of our evaluations, may reflect that plots with higher levels of tree mortality (PIPO dominated) tend to be at lower elevations and lower latitudes, where forests tend to be less productive and accumulate surface fuels more slowly (Young et al., 2020). However, as highlighted earlier, with increased rates of snag fall expected in the near-term, changes in the nature and magnitude of fuel accumulations across our study sites, particularly in stands dominated by pine species, should be anticipated. Compared to fine fuels, CWD dry out over longer time scales, which has historically made them less available to burn over the course of the fire season (Goodwin et al., 2021). Yet, with projected increasing temperatures and severe droughts (Dettinger et al., 2018), this apparent control on fuel flammability might be altered as the moisture of these larger fuels decreases while fuel aridity increase. This pulse of heavy fuels could also serve to create even more homogeneous surface fuel conditions across large areas and exacerbate conditions that lead to large, stand-replacing fires (Stephens et al., 2018).

5. Conclusions

Many studies have previously addressed the topic of fuels in Sierra Nevada forests, particularly to compare the effects of different fuel treatments on the amount and distribution of fuels, or how fuels influence fire behavior. However, a novel aspect of our study is that it captured the short-term, post-drought and pre-snag fall status of surface fuels across much of the region following a widespread tree mortality event. As noted by Hartmann et al. (2022), such unexpected events represent one of the risks climate change poses to global forest health. Thus, it is essential to gain a better understanding of both drivers of elevated tree mortality and its consequences on forest ecosystems. Our work contributes to this understanding by documenting baseline conditions essential to the stewardship of forests that could see emerging tree mortality effects.

This study was also motivated, in part, by the fact that accurate characterization of fuel loads, especially before fire occurs, is crucial to the reintroduction of fire to these fire-suppressed forests, and for the prioritization of fuels treatments across the landscape. A high proportion of the stands evaluated in our study could be extremely vulnerable to high-severity wildfires given the combination of high fuel loads and increasing frequency of weather conditions that promote fire growth such as high temperatures and severe droughts. Finally, taking advantage of the permanent status of many of the plots used in our study, we recommend continuous monitoring of fuels aiming at increasing our overall understanding of fuel dynamics and improve the quality of models used to analyze fire behavior, treatment optimization, and carbon emissions from wildfires across western Sierra Nevada forests.

6. Data and code availability

Plot-level data of surface fuels, overstory and biophysical variables, as well as the R code used during data analysis is available at https://zenodo.org/record/7770365.

CRediT authorship contribution statement

Emilio Vilanova: Investigation, Data curation, Visualization, Writing – original draft. **Leif A. Mortenson:** Data curation, Investigation, Writing – review & editing. **Lauren E. Cox:** Data curation, Writing – review & editing. **Beverly M. Bulaon:** Data curation, Writing – review & editing. **Jamie M. Lydersen:** Writing – review & editing. **Christopher J. Fettig:** Funding acquisition, Investigation, Writing – review & editing. **John J. Battles:** Funding acquisition, Investigation, Writing – review & editing. **Jodi N. Axelson:** Funding acquisition, Investigation, Writing – review & editing.

Declaration of Competing Interest

The authors declare that they have no known competing financial interests or personal relationships that could have appeared to influence the work reported in this paper.

Data availability

Plot-level data of surface fuels, overstory and biophysical variables, as well as the R code used during data analysis are available at https://zenodo.org/record/7770365.

Acknowledgments

Large field-based studies require a great deal of assistance from numerous personnel, field crews, and funding agencies. We wish to thank our UCB summer student field crews, particularly E. Kuskulis, who were instrumental in establishing the UCB plot network. We also thank D. Cluck and A. Hoffman (Forest Health Protection, USDA Forest Service), N. Foote (Oregon State University), R. Gerrard (Pacific Southwest Research Station, USDA Forest Service), M. Koontz (University of California-Davis), P. Foulk, M. Meyer and A. Wuenschel (National Forest System, USDA Forest Service), and J. Runyon (Rocky Mountain Research Station, USDA Forest Service) for their assistance with establishing the USFS plots. We also thank D. Foster (UC Berkeley) for his valuable help with the RFuels package.

Funding sources

The California Tree Mortality Data Collection Network (DX-Project) at UC Berkeley is supported, in part, by grants to J.N.A and J.J.B. from the California Department of Forestry and Fire Protection (CALFIRE), agreement No. 8CA0529; University of California Agriculture and Natural Resources (UCANR), Competitive Grant No. 17-5049 and Opportunity Grant No. 17-OP03); USDI Bureau of Land Management SA19-0013 and USDI National Park Service via California Cooperative Ecosystem Studies Unit Task Agreement P15AC01544. This research was also supported, in part, by grants from the Pacific Southwest Research Station Climate Change Competitive Grant Program to C.J.F. (PSW–2016–03, PSW–2017–02).

Appendix A. Supplementary material

Supplementary data to this article can be found online at https://doi.org/10.1016/j.foreco.2023.120945.

References

Agee, J.K., Skinner, C.N., 2005. Basic principles of forest fuel reduction treatments. For. Ecol. Manage. 211, 83–96. https://doi.org/10.1016/j.foreco.2005.01.034.

Agee, J.K., Wakimoto, R.H., Biswell, H.H., 1977. Fire and fuel dynamics of Sierra Nevada conifers. For. Ecol. Manage. 1, 255–265.

Alboukadel, K., Mundt, F., 2020. factoextra: Extract and Visualize the Results of Multivariate Data Analyses. R package version 1, 7.

Axelson, J., Battles, J., Bulaon, B., Cluck, D., Cousins, S., Cox, L., Estes, B., Fettig, C., Hefty, A., Hishinuma, S., Hood, S., Kocher, S., McMahon, D., Mortenson, L., Koltunov, A., Kuskulis, E., Poloni, A., Ramirez, C., Restaino, C., Safford, H., Slaton, M., Smith, S., Tubbesing, C., Wayman, R., Young, D., 2019. The California Tree Mortality Data Collection Network - Enhanced communication and collaboration among scientists and stakeholders. Calif. Agric. 73, 55–62. https://doi.org/10.3733/ca.2019a0001.

Banwell, E.M., Varner, J.M., 2014. Structure and composition of forest floor fuels in long-unburned Jeffrey pine-white fir forests of the Lake Tahoe Basin, USA. Int. J. Wildland Fire 23, 363–372. https://doi.org/10.1071/WF13025.

Barton, K., 2022. Package 'MuMIn' Version 1.47.1 73.

Brooks, M., Kristensen, K., van Benthem, K., Magnusson, A., Berg, C.W., Nielsen, A., Skaug, H., Machler, M., Bolker, B., 2017. glmmTMB Balances speed and flexibility among packages for zero-inflated generalized linear mixed modeling. The R Journal 9, 378–400.

Brown, J.K., 1974. Handbook for inventorying downed woody material. USDA Forest Service General Technical Report INT-16, Ogden, Utah.

Burnham, K., P., Anderson, D., R., 2002. Model selection and multimodel inference: a practical information-theoretic approach, 2nd ed. Springer-Verlag New York, Inc.

Byer, S., Jin, Y., 2017. Detecting drought-induced tree mortality in Sierra Nevada forests with time series of satellite data. Remote Sens. (Basel) 9, 14–17. https://doi.org/10.3390/rs9090929.

Cansler, C.A., Swanson, M.E., Furniss, T.J., Larson, A.J., Lutz, J.A., 2019. Fuel dynamics after reintroduced fire in an old-growth Sierra Nevada mixed-conifer forest. Fire Ecol. 15 https://doi.org/10.1186/s42408-019-0035-y.

Collins, B.M., Lydersen, J.M., Fry, D.L., Wilkin, K., Moody, T., Stephens, S.L., 2016. Variability in vegetation and surface fuels across mixed-conifer-dominated landscapes with over 40 years of natural fire. For. Ecol. Manage. 381, 74–83. https://doi.org/10.1016/j.foreco.2016.09.010.

Cova, G., Kane, V.R., Prichard, S., North, M., Cansler, C.A., 2023. The outsized role of California's largest wildfires in changing forest burn patterns and coarsening ecosystem scale. For. Ecol. Manage. 528, 120620 https://doi.org/10.1016/j.foreco.2022.120620.

Dettinger, M., Alpert, H., Battles, J.J., Kusel, J., Safford, H., Fougeres, D., Knight, C., Miller, L., Sawyer, S., 2018. Sierra Nevada Summary Report. California's Fourth Climate Change Assessment, State of California.

Dore, S., Fry, D.L., Collins, B.M., Vargas, R., York, R.A., Stephens, S.L., 2016. Management impacts on carbon dynamics in a Sierra Nevada mixed conifer forest. PLoS One 11, 1–22. https://doi.org/10.1371/journal.pone.0150256.

Fettig, C.J., Mortenson, L.A., Bulaon, B.M., Foulk, P.B., 2019. Tree mortality following drought in the central and southern Sierra Nevada, California, U.S. For. Ecol. Manage. 432, 164–178. https://doi.org/10.1016/j.foreco.2018.09.006.

Flint, L.E., Flint, A.L., Thorne, J.H., Boynton, R., 2013. Fine-scale hydrologic modeling for regional landscape applications: the California Basin Characterization Model development and performance. Ecol. Process. 2, 25. https://doi.org/10.1186/2192-1709-2-25.

Fosberg, M.A., 1970. Drying rates of heartwood below fiber saturation. For. Sci. 16, 57–63. https://doi.org/10.1093/forestscience/16.1.57.

Foster, D.E., Stephens, S.L., Moghaddas, J., van Wagtendonk, J.W., 2018. Rfuels: Forest Fuels from Brown's Transects. Available at: https://github.com/danfosterfire/Rfuels.

Frandsen, W.H., 1987. The influence of moisture and mineral soil on the combustion limits of smoldering forest duff. Can. J. For. Res. 17, 1540–1544. https://doi.org/10.1139/x87-236.

Gillson, L., Whitlock, C., Humphrey, G., 2019. Resilience and fire management in the Anthropocene. Ecol. Soc. 24 https://doi.org/10.5751/ES-11022-240314.

Goodwin, M.J., Zald, H.S.J., North, M.P., Hurteau, M.D., 2021. Climate-Driven tree mortality and fuel aridity increase wildfire's potential heat flux. Geophys. Res. Lett. 48, e2021GL094954 https://doi.org/10.1029/2021GL094954.

Gotelli, N., Ellison, A., 2004. The Analysis of Multivariate Data. In: Gotelli, N.J., Ellison, A. (Eds.), A Primer of Ecological Statistics. Sinauer, Sunderland, MA, USA, pp. 381–445.

Goulden, M.L., Bales, R.C., 2019. California forest die-off linked to multi-year deep soil drying in 2012–2015 drought. Nat. Geosci. 12 https://doi.org/10.1038/s41561-019-0388-5.

Grayson, L.M., Cluck, D.R., Hood, S.M., 2019. Persistence of fire-killed conifer snags in California, USA. Fire Ecology 15, 1–14. https://doi.org/10.1186/s42408-018-0007-7.

Hagmann, R.K., Hessburg, P.F., Prichard, S.J., Povak, N.A., Brown, P.M., Fulé, P.Z., Keane, R.E., Knapp, E.E., Lydersen, J.M., Metlen, K.L., Reilly, M.J., Sánchez Meador, A.J., Stephens, S.L., Stevens, J.T., Taylor, A.H., Yocom, L.L., Battaglia, M.A., Churchill, D.J., Daniels, L.D., Falk, D.A., Henson, P., Johnston, J.D., Krawchuk, M.A., Levine, C.R., Meigs, G.W., Merschel, A.G., North, M.P., Safford, H.D., Swetnam, T. W., Waltz, A.E.M., 2021. Evidence for widespread changes in the structure, composition, and fire regimes of western North American forests. Ecol. Appl. 31 https://doi.org/10.1002/eap.2431.

Hall, S.A., Burke, C., Hobbs, N.T., 2006. Litter and dead wood dynamics in ponderosa pine forests along a 160-year chronosequence. Ecol. Appl. 16, 2344–2355. https://doi.org/10.1890/1051-0761(2006)016[2344:LADWDI]2.0.CO;2.

Harmon, M.E., Sexton, J.O., 1996. Guidelines for measurements of woody detritus in forest ecosystems. University of Washington, U.S LTER Network Office., Seattle.

Hartmann, H., Bastos, A., Das, A.J., Esquivel-Muelbert, A., Hammond, W.M., Martínez-Vilalta, J., McDowell, N.G., Powers, J.S., Pugh, T.A.M., Ruthrof, K.X., Allen, C.D., 2022. Climate change risks to global forest health: Emergence of unexpected events of elevated tree mortality worldwide. Annu. Rev. Plant Biol. 73, 673–702. https://doi.org/10.1146/annurev-arplant-102820-012804.

Johnson, J.B., Omland, K.S., 2004. Model selection in ecology and evolution. Trends Ecol. Evol. 19, 101–108. https://doi.org/10.1016/j.tree.2003.10.013.

Kareiva, P., Carranza, V., 2018. Existential risk due to ecosystem collapse: Nature strikes back. Futures 102, 39–50. https://doi.org/10.1016/j.futures.2018.01.001.

Keane, R.E., 2013. Describing wildland surface fuel loading for fire management: A review of approaches, methods and systems. Int. J. Wildland Fire 22, 51–62. https://doi.org/10.1071/WF11139.

Keane, R.E., Gray, K., 2013. Comparing three sampling techniques for estimating fine woody down dead biomass. Int. J. Wildland Fire 22, 1093–1107.

Kennedy, M.C., Johnson, M.C., Harrison, S.C., 2021. Model predictions of post-wildfire woody fuel succession and fire behavior are sensitive to fuel dynamics parameters. For. Sci. 67, 30–42. https://doi.org/10.1093/forsci/fxaa036.

Khun, M., 2020. caret: Classification and Regression Training. R package version 6.0-86.

Knapp, E.E., Keeley, J.E., Ballenger, E.A., Brennan, T.J., 2005. Fuel reduction and coarse woody debris dynamics with early season and late season prescribed fire in a Sierra Nevada mixed conifer forest. For. Ecol. Manage. 208, 383–397. https://doi.org/10.1016/j.foreco.2005.01.016.

Low, K.E., Collins, B.M., Bernal, A., Sanders, J.E., Pastor, D., Manley, P., White, A.M., Stephens, S.L., 2021. Longer-term impacts of fuel reduction treatments on forest structure, fuels, and drought resistance in the Lake Tahoe Basin. For. Ecol. Manage. 479, 118609 https://doi.org/10.1016/j.foreco.2020.118609.

Lutz, J.A., Struckman, S., Furniss, T.J., Cansler, C.A., Germain, S.J., Yocom, L.L., McAvoy, D.J., Kolden, C.A., Smith, A.M.S., Swanson, M.E., Larson, A.J., 2020. Large-diameter trees dominate snag and surface biomass following reintroduced fire. Ecol. Process. 9 https://doi.org/10.1186/s13717-020-00243-8.

Lydersen, J.M., Collins, B.M., Coppoletta, M., Jaffe, M.R., Northrop, H., Stephens, S.L., 2019. Fuel dynamics and reburn severity following high-severity fire in a Sierra Nevada, USA, mixed-conifer forest. Fire Ecology 15. https://doi.org/10.1186/s42408-019-0060-x.

Lydersen, J.M., Collins, B.M., Ewell, C.M., Reiner, A.L., Fites, J.A., Dow, C.B., Gonzalez, P., Saah, D.S., Battles, J.J., 2014. Using field data to assess model predictions of surface and ground fuel consumption by wildfire in coniferous forests of California. J. Geophys. Res. Biogeo. 119, 223–235. https://doi.org/10.1002/2013JG002475.Received.

Lydersen, J.M., Collins, B.M., Knapp, E.E., Roller, G.B., Stephens, S., 2015. Relating fuel loads to overstorey structure and composition in a fire-excluded Sierra Nevada mixed conifer forest. Int. J. Wildland Fire 24, 484–494. https://doi.org/10.1071/WF13066.

Lydersen, J.M., North, M., 2012. Topographic variation in structure of mixed-conifer forests under an active fire regime. Ecosystems 15, 1134–1146. https://doi.org/10.1007/s10021-012-9573-8.

Martinez, A.J., Meddens, A.J.H., Kolden, C.A., Strand, E.K., Hudak, A.T., 2019. Characterizing persistent unburned islands within the Inland Northwest USA. Fire Ecology 15, 20. https://doi.org/10.1186/s42408-019-0036-x.

Moritz, M.A., Morais, M.E., Summerell, L.A., Carlson, J.M., Doyle, J., 2005. Wildfires, complexity, and highly optimized tolerance. Proc. Natl. Acad. Sci. U.S.A. 102, 17912–17917. https://doi.org/10.1073/pnas.0508985102.

Nakagawa, S., Schielzeth, H., 2013. A general and simple method for obtaining R2 from generalized linear mixed-effects models. Methods Ecol. Evol. 4, 133–142. https://doi.org/10.1111/j.2041-210x.2012.00261.x.

North, M., Tompkins, R.E., Bernal, A.A., Collins, B.M., Stephens, S.L., York, R.A., 2022. Operational resilience in western US frequent-fire forests. For. Ecol. Manage. 507, 120004 https://doi.org/10.2139/ssrn.3967014.

North, M.P., Hurteau, M.D., 2011. High-severity wildfire effects on carbon stocks and emissions in fuels treated and untreated forest. For. Ecol. Manage. 261, 1115–1120. https://doi.org/10.1016/j.foreco.2010.12.039.

Parks, S.A., Parisien, M.-A., Miller, C., Dobrowski, S.Z., 2014. Fire Activity and Severity in the Western US Vary along Proxy Gradients Representing Fuel Amount and Fuel Moisture. PLoS One 9, e99699.

Parks, S.A., Abatzoglou, J.T., 2020. Warmer and drier fire seasons contribute to increases in area burned at high severity in western US forests From 1985 to 2017. Geophys. Res. Lett. 47, 1–10. https://doi.org/10.1029/2020GL089858.

Prichard, S.J., Kennedy, M.C., Andreu, A.G., Eagle, P.C., French, N.H., Billmire, M., 2019. Next-generation biomass mapping for regional emissions and carbon inventories: incorporating uncertainty in wildland fuel characterization. J. Geophys. Res. Biogeo. 124, 3699–3716. https://doi.org/10.1029/2019JG005083.

Prichard, S.J., Rowell, E.M., Hudak, A.T., Keane, R.E., Loudermilk, E.L., Lutes, D.C., Ottmar, R.D., Chappell, L.M., Hall, J.A., Hornsby, B.S., 2022. Fuels and Consumption. In: Peterson, D.L., McCaffrey, S.M., Patel-Weynand, T. (Eds.), Wildland Fire Smoke in the United States: A Scientific Assessment. Springer International Publishing, Cham, pp. 11–49. https://doi.org/10.1007/978-3-030-87045-4_2.

PRISM Climate Group, 2020. PRISM Gridded climate data [WWW Document]. URL http://prism.oregonstate.edu (accessed 9.25.20).

R Core Team, 2022. R: A language and environment for statistical computing. R Foundation for Statistical Computing, Vienna, Austria. URL https://www.R-project.org/.
Raphael, M.G., Morrison, M.L., 1987. Decay and dynamics of snags in the Sierra Nevada, California. For. Sci. 33, 774–783. https://doi.org/10.1093/forestscience/33.3.774.
Restaino, C., Young, D.J.N., Estes, B., Gross, S., Wuenschel, A., Meyer, M., Safford, H., 2019. Forest structure and climate mediate drought-induced tree mortality in forests of the Sierra Nevada, USA. Ecol. Appl. 29 https://doi.org/10.1002/eap.1902.
Robbins, Z.J., Xu, C., Aukema, B.H., Buotte, P.C., Chitra-Tarak, R., Fettig, C.J., Goulden, M.L., Goodsman, D.W., Hall, A.D., Koven, C.D., Kueppers, L.M., Madakumbura, G.D., Mortenson, L.A., Powell, J.A., Scheller, R.M., 2022. Warming increased bark beetle-induced tree mortality by 30% during an extreme drought in California. Glob. Chang. Biol. 28, 509–523. https://doi.org/10.1111/gcb.15927.
Ryan, K.C., Frandsen, W.H., 1991. Basal injury from smoldering fires in mature Pinus ponderosa (Laws). Int. J. Wildland Fire 1, 107–118.
Ryan, K.C., Knapp, E.E., Varner, J.M., 2013. Prescribed fire in North American forests and woodlands: history, current practice, and challenges. Front. Ecol. Environ. 11, e15–e24. https://doi.org/10.1890/120329.
Safford, H.D., Stevens, J.T., 2017. Natural range of variation for yellow pine and mixed-conifer forests in the Sierra Nevada, southern Cascades, and Modoc and Inyo National Forests, California, USA. Gen. Tech. Rep. PSW-GTR-256. Albany, CA: U.S. Department of Agriculture, Forest Service, Pacific Southwest Research Station. 229 p.
Seidl, R., Spies, T.A., Peterson, D.L., Stephens, S.L., Hicke, J.A., 2016. Searching for resilience: Addressing the impacts of changing disturbance regimes on forest ecosystem services. J. Appl. Ecol. 53, 120–129. https://doi.org/10.1111/1365-2664.12511.
Seidl, R., Thom, D., Kautz, M., Martin-Benito, D., Peltoniemi, M., Vacchiano, G., Wild, J., Ascoli, D., Petr, M., Honkaniemi, J., Lexer, M.J., Trotsiuk, V., Mairota, P., Svoboda, M., Fabrika, M., Nagel, T.A., Reyer, C.P.O., 2017. Forest disturbances under climate change. Nat. Clim. Chang. 7, 395–402. https://doi.org/10.1038/nclimate3303.
Shive, K.L., Wuenschel, A., Hardlund, L.J., Morris, S., Meyer, M.D., Hood, S.M., 2022. Ancient trees and modern wildfires: Declining resilience to wildfire in the highly fire-adapted giant sequoia. For. Ecol. Manage. 511, 120110 https://doi.org/10.1016/J.FORECO.2022.120110.
Steel, Z.L., Jones, G.M., Collins, B.M., Green, R., Koltunov, A., Purcell, K.L., Sawyer, S.C., Slaton, M.R., Stephens, S.L., Stine, P., Thompson, C., 2022. Mega-disturbances cause rapid decline of mature conifer forest habitat in California. Ecol. Appl. https://doi.org/10.1002/eap.2763.
Steel, Z.L., Safford, H.D., Viers, J.H., 2015. The fire frequency-severity relationship and the legacy of fire suppression in California forests. Ecosphere 6, art8. https://doi.org/10.1890/es14-00224.1.
Stephens, S.L., Collins, B.M., Fettig, C.J., Finney, M.A., Hoffman, C.M., Knapp, E.E., North, M.P., Safford, H., Wayman, R.B., 2018. Drought, tree mortality, and wildfire in forests adapted to frequent fire. Bioscience 68, 77–88. https://doi.org/10.1093/biosci/bix146.
Stephens, S.L., Collins, B.M., Roller, G., 2012. Fuel treatment longevity in a Sierra Nevada mixed conifer forest. For. Ecol. Manage. 285, 204–212. https://doi.org/10.1016/j.foreco.2012.08.030.
Stephens, S.L., Finney, M.A., 2002. Prescribed fire mortality of Sierra Nevada mixed conifer tree species: effects of crown damage and forest floor combustion. For. Ecol. Manage. 162, 261–271. https://doi.org/10.1016/S0378-1127(01)00521-7.
Stephens, S.L., Martin, R.E., Clinton, N.E., 2007. Prehistoric fire area and emissions from California's forests, woodlands, shrublands, and grasslands. For. Ecol. Manage. 251, 205–216. https://doi.org/10.1016/j.foreco.2007.06.005.
Stephens, S.L., Moghaddas, J.J., 2005. Experimental fuel treatment impacts on forest structure, potential fire behavior, and predicted tree mortality in a California mixed conifer forest. For. Ecol. Manage. 215, 21–36. https://doi.org/10.1016/j.foreco.2005.03.070.
Stevens, D.L., Olsen, A.R., 2004. Spatially balanced sampling of natural resources. J. Am. Stat. Assoc. 99, 262–278. https://doi.org/10.1198/016214504000000250.
Stevens, J.T., Collins, B.M., Miller, J.D., North, M.P., Stephens, S.L., 2017. Changing spatial patterns of stand-replacing fire in California conifer forests. For. Ecol. Manage. 406, 28–36. https://doi.org/10.1016/j.foreco.2017.08.051.
Taylor, A.H., Vandervlugt, A.M., Maxwell, R.S., Beaty, R.M., Airey, C., Skinner, C.N., 2014. Changes in forest structure, fuels and potential fire behaviour since 1873 in the Lake Tahoe Basin, USA. Appl. Veg. Sci. 17, 17–31. https://doi.org/10.1111/avsc.12049.
Tibshirani, R., Walther, G., Hastie, T., 2001. Estimating the number of clusters in a data set via the gap statistic. J. R. Stat. Soc. Ser. B (Stat Methodol.) 63, 411–423. https://doi.org/10.1111/1467-9868.00293.
USFS, 2009. Existing Vegetation - CALVEG, [ESRI personal geodatabase]. Accessed on March 10th, 2023.
Vaillant, N.M., Fites-Kaufman, J., Reiner, A.L., Noonan-Wright, E.K., Dailey, S.N., 2009. Effect of fuel treatments on fuels and potential fire behavior in California, USA, national forests. Fire Ecology 5, 14–29. https://doi.org/10.4996/fireecology.0502014.
Van de Water, K., North, M., 2011. Stand structure, fuel loads, and fire behavior in riparian and upland forests, Sierra Nevada Mountains, USA: a comparison of current and reconstructed conditions. For. Ecol. Manage. 262, 215–228. https://doi.org/10.1016/j.foreco.2011.03.026.
van Wagdendonk, J.W., Benedict, J.M., Sydoriak, W.M., 1996. Physical properties of woody fuel particles of Sierra Nevada conifers. Int. J. Wildland Fire 6, 117–123.
van Wagtendonk, J.W., Benedict, J.M., Sydoriak, W.M., 1998. Fuel bed characteristics of Sierra Nevada conifers. West. J. Appl. For. 13, 73–84. https://doi.org/10.1093/wjaf/13.3.73.
Wang, J.A., Randerson, J.T., Goulden, M.L., Knight, C.A., Battles, J.J., 2022. Losses of tree cover in California driven by increasing fire disturbance and climate stress. AGU Advances 3, e2021AV000654. https://doi.org/10.1029/2021AV000654.
Weise, D., Gelobter, A., Haase, S., Sackett, S., 1997. Photo series for quantifying fuels and assessing fire risk in Giant Sequoia groves. Gen. Tech. Rep. PSW-GTR-163. Albany, CA: Pacific Southwest Research Station, Forest Service, U.S. Department of Agriculture; 49 p.
Williams, A.P., Cook, B.I., Smerdon, J.E., 2022. Rapid intensification of the emerging southwestern North American megadrought in 2020–2021. Nat. Clim. Chang. 12, 232–234. https://doi.org/10.1038/s41558-022-01290-z.
Williams, A.P., Cook, E.R., Smerdon, J.E., Cook, B.I., Abatzoglou, J.T., Bolles, K., Baek, S.H., Badger, A.M., Livneh, B., 2020. Large contribution from anthropogenic warming to an emerging North American megadrought. Science 368, 314–318. https://doi.org/10.1126/science.aaz9600.
Young, D.J.N., Meyer, M., Estes, B., Gross, S., Wuenschel, A., Restaino, C., Safford, H.D., 2020. Forest recovery following extreme drought in California, USA: natural patterns and effects of pre-drought management. Ecol. Appl. 30, e02002.
Young, D.J.N., Stevens, J.T., Earles, J.M., Moore, J., Ellis, A., Jirka, A.L., Latimer, A.M., 2017. Long-term climate and competition explain forest mortality patterns under extreme drought. Ecol. Lett. 20, 78–86. https://doi.org/10.1111/ele.12711.